Imbalanced nitrogen–phosphorus input alters soil organic carbon storage and mineralisation in a salt marsh

Juanyong Li [a,b], Guangxuan Han [a,c,d,*], Guangmei Wang [a,c,d,*], Xiaoling Liu [a], Qiqi Zhang [a,e], Yawen Chen [a,e], Weimin Song [a,c], Wendi Qu [a,e], Xiaojing Chu [a,c], Peiguang Li [a,c]

[a] CAS Key Laboratory of Coastal Environmental Processes and Ecological Remediation, Yantai Institute of Coastal Zone Research (YIC), Chinese Academy of Sciences (CAS), Shandong Key Laboratory of Coastal Environmental Processes, YICCAS, Yantai Shandong, 264003, PR China
[b] Research Institute for Big Data & Internet Innovation, Hunan University of Technology and Business, Changsha 410205, PR China
[c] Yellow River Delta Field Observation and Research Station of Coastal Wetland Ecosystem, Chinese Academy of Sciences, PR China
[d] Center for Ocean Mega-science, Chinese Academy of Sciences, 7 Nanhai Road, Qingdao 266071, PR China
[e] University of Chinese Academy of Sciences, Beijing 100049, PR China

ABSTRACT

A large imbalance in soil nitrogen (N) and phosphorus (P) inputs induced by anthropogenic activities is anticipated to profoundly influence soil carbon (C) budgets in salt marshes. In this study, we hypothesized that imbalances in the nitrogen–phosphorus (N–P) input would result in the nonlinear response of soil organic carbon (SOC) content, fractions and mineralization to the N–P input ratio. We applied three N–P input ratios (low (5:1), medium (15:1), high (45:1)) in a salt marsh of the Yellow River Delta (YRD) for four years (in which N added increased from 8.67 to 26.01 g N m^{-2} y^{-1} and P added decreased from 1.73 to 0.58 g P m^{-2} y^{-1}) and quantified their impacts on SOC fractions and SOC mineralisation. The control treatment did not receive fertilization. The results showed that the N and P input led to overall increases in the availability of soil nutrients (i.e., inorganic N (IN) and available P (AP)), stimulation of plant biomass and changes of microbial community structure (i.e., γ- and δ-Proteobacteria and Acidobacteria). N and P input increased soil dissolved organic carbon (DOC) and decreased aromatic DOC components through improving N availability and stimulating plant growth. Notably, though, there may be a threshold N–P input ratio between 15:1 and 45:1 that, once crossed, triggers the loss of SOC. Appropriate increase in N availability induced by low and medium N-P input ratios would stimulate the SOC mineralisation. However, excessive N-P input ratio would reduce SOC mineralisation. Path analysis indicated that N–P input ratios dominantly regulate SOC mineralisation by changing soil DOC and microbial biomass (MBC)contents and microbial community structure. Thus, we speculate that the continuous increase in N input causes a growing N–P imbalance that reduces SOC stocks, despite a reduction in SOC mineralisation.

1. Introduction

Coastal wetland has a disproportionate impact on the global carbon (C) cycle. Despite occupying a mere 0.2% of the Earth's surface area, coastal wetlands hold 55% of the total amount of C absorbed and fixed by organisms on Earth (Kirwan and Mudd, 2012; Nellemann et al., 2009). Soil C is by far the largest C sink in the coastal wetland ecosystems, which is vital for buffering increasing levels of atmospheric CO_2 (Chmura et al., 2003; Jian et al., 2016). The dynamics of soil C sinks in coastal wetlands are founded on the balance between plant-derived C inputs and the outputs of C, primarily via the microbial decomposition of soil organic carbon (SOC) and leaching of dissolved organic carbon (DOC) (Cao et al., 2019; Vesterdal et al., 2012; Wieder et al., 2015). As the coastal wetland represents one of the most sensitive ecosystems on Earth, minor shifts in the dynamics of these environments can greatly alter soil C storage, which will influence global greenhouse gas emissions (Gao et al., 2014; Zhou et al., 2019).

Increased anthropogenic nitrogen (N) input to coastal wetland ecosystems has created a severe imbalance between N and phosphorus (P) and likely affected soil biogeochemical C cycles in these ecosystems (Peng et al., 2019; Peñuelas et al., 2013). The effects of N and P input on SOC accumulation via changes in the inputs and outputs of SOC have

been widely investigated (Schleuss et al., 2019; Pastore et al., 2017; Stiles et al., 2017). Some studies have shown that relatively short-term high N and low P input tend to increase the N-uptake of plants and stimulate plant growth thereby increasing soil C sequestration (Hill and Roberts, 2017; Peng et al., 2019). However, a great deal of research has demonstrated that high N: P ratios negatively impact plant growth, especially belowground biomass allocation (Deegan et al., 2012; Chen et al., 2017; Wang et al., 2019). In addition, excessive P addition was also unfavorable for improving N availability and plant growth since the efficiency of applied P was low (Sonmez et al., 2016). Some simulations have even shown that continuously imbalanced nitrogen–phosphorus (N–P) input could shift ecosystems from C sinks to C sources by the end of this century (Sun et al., 2017; Wieder et al., 2015). Appropriate nutrients input can stimulate the decomposition of SOC through increasing the production of soil labile organic C (i.e., DOC and microbial biomass carbon (MBC)) (Hasselquist et al., 2012; Davies et al., 2017). Nevertheless, P-limitation induced by N-saturation has repeatedly been shown to suppress SOC mineralisation because of reductions in oxidative enzymes and microbial N mining (Ramirez et al., 2012; Schleuss et al., 2019). For example, the balanced addition of N and P was found to stimulate soil respiration by promoting labile C and stimulating copiotrophic microbial communities with high growth rates and fast turn-over (Pascault et al., 2013; Schleuss et al., 2019; Wei et al., 2020). Furthermore, some copiotrophic taxa were stimulated by the singular addition of N, while some N-sensitive classes were inhibited (Mannisto et al., 2016; Tahovska et al., 2020). Such results have led to researchers to speculate that SOC accumulation and biogeochemical cycles may respond nonlinearly to N-P input ratio.

In nonlinear responses, thresholds represent critical values beyond which ecosystem functions may change (Cheng et al., 2017). It is remarkable that the threshold of N–P input ratio is likely inconsistent across different ecosystems and regions. Moreover, the thresholds for the inputs and outputs of SOC are also appear to be inconsistent due to the differing degrees of N-saturation that plants and microbes can endure (Gueyewell and Gessner, 2009; Luo et al., 2016; Penuelas et al., 2013). Thus, understanding the responses of SOC fractions and mineralisation process to N–P input ratios are vital for managing the function of soil C sink of coastal wetlands under the influence of global climate change. In this study, we hypothesized that the concentration of SOC fractions and SOC mineralisation responded nonlinearly to the N-P input ratio. To test our hypothesis, we conducted a field experiment that simulated different N-P input ratios in a salt marsh of the Yellow River Delta (YRD) to elucidate the impacts of N–P input ratio on SOC content and fractions. We also conducted a soil incubation experiment to quantify SOC mineralisation by measuring CO_2 under different N–P input ratios. Our objectives were to: (1) identify the responses of SOC fractions to different N–P input ratio, (2) investigate the response of SOC mineralisation to different N–P input ratio, (3) explore the potential linkages between changes in SOC fractions, SOC mineralisation, soil chemical properties and microbial community structure under different N–P input ratio.

2. Materials and methods

2.1. Study area

The long-term nutrient addition experiment was conducted in a salt marsh (37°45′52″ N, 118°58′52″ E) of the YRD, Shandong Province, China. The local climate is a warm-temperate and continental monsoon climate. Mean precipitation amounts to 560 mm year^{-1}, and most rainfall occurs between June and September. The mean annual temperature is 12.9 °C, while the monthly minimum and maximum temperatures range between −2.8 °C and 26.7 °C, respectively (Han et al., 2018). This study site is dominated by halophytes, such as *Suaeda glauca, Suaeda salsa, Phragmites australis,* and *Tamarix chinensis* (Han et al., 2018; Liu et al., 2019). Saline soil is the main soil types. The texture is

sandy clay loam and the soil is well drained (Nie et al., 2009). In recent years, this area has experienced an increasing input of N since the inorganic N (IN) content in coastal water was continuously increasing, while that of P remains low, which has resulted in an increasing imbalance in the input of N and P (Li et al., 2017). Ambient IN deposition (wet + dry) at this site averages ~ 2.26 g N m^{-2} year^{-1} (Yu et al., 2014). Soil properties of the plots before the start of the experiments were showed in Table S1.

2.2. Field experiment

Field nutrient addition experiment was established in July of 2014 and N and P application began in 2015. The experiments were designed with one control treatment and three N–P input ratios including low (5:1), medium (15:1) and high (45:1). These treatments simulated N limited, balanced input and P limited, respectively. The balanced input treatment was set to 15:1N/P because plants are likely to be equally limited by N and P in this ratio (Koerselman and Meuleman, 1996). Each treatment had four replicated plots (3.5 m × 3.5 m). We selected a block (40 m × 35 m) with fairly uniform vegetation composition and soil physio-chemical properties within the research station (Liu et al., 2019). All twelve plots were randomly distributed within each block. Considering the ambient N deposition and other N input sources, we defined 5 g N m^{-2} year^{-1} as the background value of N input and tripled the value to 15 g N m^{-2} year^{-1} as the annual input of N for the medium N–P input ratio. The annual input of N and P for all input ratios were calculated as proposed by Gusewell (2005) and Liu et al. (2019):

$$N(g) = L(g) \cdot \sqrt{N:P}$$

$$N(g) = L(g)/\sqrt{N:P}$$

where N (g) and P (g) are the input amount of N and P, respectively. And *L (g)* is the geometric average of the amounts of N and P applied.

The amounts of four different treatments with respective N and P addition rates are provided in Table 1. N was applied as urea and P as NaH_2PO_4. Fertilization was performed at the corresponding concentrations using a backpack sprayer with one-second of the annual dose in early April (germination stage) and late June (vigorous growth stage) every year. The fertilizers were dissolved in 6 L of water and applied to the plots and the control treatment received an equal amount of water. Plant biomass was harvested each year for 2015, 2017 and 2018 in early August (peak biomass season). An inundation event in July 2016 caused the loss of plant biomass and hindered its harvest.

2.3. Soil sampling

In late March of 2019 (before initial fertilization in early April of 2019), five sampling points were randomly selected in each plot. Fresh litter was cleared from these points to facilitate the collection of soil samples from the first 10 cm of the soil profile. All soil samples were transferred under field moist conditions to the laboratory. Samples were first passed through a 4-mm sieve to ensure homogenization with minimal disruption to the soil structure; then, all roots and coarse soil fragments were removed. Each sample was subsequently divided into four sub-samples. One fresh sub-sample was used for a SOC mineralisation incubation experiment. Another fresh sub-sample was

Table 1
Annual amount of nitrogen and phosphorus applied at the treatments (g m^{-2} y^{-1}).

N: P	N	P
Control	0	0
5: 1	8.67	1.73
15: 1	15.00	1.00
45: 1	26.01	0.58

refrigerated at 4 °C and used to analyse the microbial biomass within one week. A third sub-sample was stored at −80 °C for later measurements of microbial community composition. The fourth sub-sample was used to determine soil chemical properties following air drying.

2.4. Soil and microbial analyses

The SOC storage (SOC, DOC, specific ultraviolet absorbance at 254 nm ($SUVA_{254}$) and MBC) was determined. The SOC content was measured using an elemental analyzer (Vario MACRO cube, Elementar Analysensysteme, Germany) after pretreated with hydrochloric acid (HCl, 1 mol/L) for inorganic C removal. The DOC content was measured using a TOC-VCSN analyzer (Shimadzu Scientific Instrument, Columbia, MD). Subsamples of the DOC were used to analyse the $SUVA_{254}$ for determination of the aromaticity (Kalbitz et al., 2003). The $SUVA_{254}$ was measured using a T6 UV spectrophotometer (Beijing Purkinje General Instrument Co Ltd., China), and the MBC was measured using a chloroform fumigation-extraction method (Vance et al., 1987). Meanwhile, the following soil chemical properties were determined: pH, salinity, IN (defined as NH_4^+ - N + NO_3^- - N), available P (AP), microbial biomass nitrogen (MBN) and total carbon (TC). The pH was determined using a glass electrode (soil: water = 1: 5). Soil electrical conductivity (EC) was measured as a proxy for soil salinity in a 1:5 soil: deionized water suspension with an EC meter. For soil NH_4^+-N and NO_3^-N measurements, 3 g of soil (dry mass) was extracted in 15 mL 2 mol L^{-1} potassium chloride (KCl) solution, and then analysed with a continuous flow analyzer (FIA-Lab, Medizin and Labortechnik Engineering GmbH, Germany). The AP content were analysed using a T6 UV spectrophotometer (Beijing Purkinje General Instrument Co Ltd., China) through the molybdenum blue method after extracted by 0.5 mol L^{-1} $NaHCO_3$ (pH = 8.5). The MBN was measured via chloroform fumigation-extraction method. The TC content was measured using an elemental analyzer (Vario MACRO cube, Elementar Analysensysteme, Germany). SOC storage and soil chemical properties were quantified at the Yantai Institute of Coastal Wetlands, Chinese Academy of Sciences (Yantai, China).

Analysis of microbial community structure: Total DNA extraction was conducted using a PowerSoil DNA Isolation Kit (MO BIO Laboratories, Inc., USA) and stored at −20 °C. The primers 341F and 806R were used to target the bacterial 16S rRNA gene in V3–V4 fragments, which has been used effectively to distinguish functional microorganisms in previous studies (Xiao et al., 2019). Reactions (50 μl) were performed with 25 μl of 2 × Primer Taq (TaKaRa, RR902A), 1 μl forward primer (10 mM), 1 μl of reverse primer (10 mM), 3 μl of g-DNA, 20 μl of nuclease-free water. The thermal cycling conditions were as follows: 94 °C for 5 min, followed by 31 cycles of 94 °C for 30 s, 52 °C for 30 s and 72 °C for 45 s, followed by 72 °C for 10 min, and finally held at 72 °C before purification. The PCR products were analysed by gel electrophoresis. Pyrosequencing was performed on a MiSeq platform. We used Trimmomatic-0.33 for data quality control and the filtration of the raw sequence reads. After discarding the reads identified as putative chimaeras by MOTHUR (a project seeks to develop a single piece of open-source, expandable software to fill the bioinformatics needs of the microbial ecology community). For the degree of similarity between the sequences, ≥97% was defined as the threshold to obtain operational taxonomic units (OTUs), which were identified to the species level. Taxonomic assignments were achieved using UCLUST (UCLUST-1.2.22) method with a similarity of 0.5. Finally, the Greengenes OTU database (gg_13_8_otus, http://qiime.org/home_static/dataFiles.html) was mined for reference sequences.

2.5. Incubation experiments to quantify SOC mineralisation

Fresh soils (equivalent to 100 g oven dried soil) were separately weighed in 1 L sealed jars and deionized water was added to each incubation container to obtain a final soil water content of 60% of the water holding capacity. The jars were weighed daily to ensure that the soil moisture was remained at 60% of the water holding capacity. All jars were incubated at 25 °C for 90 days. Soil CO_2 efflux was determined on day 1, 3, 5, 7, 9, 11, 14, 17, 20, 23, 26, 30, 35,40, 45, 50, 55, 60, 65, 70, 75, 80, 85 and 90 of the incubation periods. For gas sampling, the jars were first flushed with air for approximately 20 min and then, sealed with a three-way valve and allowed to accumulate CO_2 for 24 h. The headspace gas was drawn using a 50-mL syringe equipped with a three-way valve. After sampling, the jars were left open to maintain aerobic conditions. The collected gas was analysed using a gas chromatograph (7890, Agilent Technologies, Inc., USA) within 12 h after sampling. The mean SOC mineralisation rate (mg CO_2-C kg^{-1} soil d^{-1}) was determined daily.

2.6. Statistical analyses

One-way analysis of variance (ANOVA) based on the least significant difference (LSD) ($p < 0.05$) was used to determine the effects of treatments on cumulative SOC mineralisation, soil DOC concentration, the $SUVA_{254}$ of soil DOC, soil properties, plant biomass and microbial community structure (relative abundance, α-diversity). The plant biomass in each treatment indicated the average of 2015, 2017 and 2018. Two measures of α-diversity were calculated to assess the biodiversity of microbial communities at different N–P input ratio treatments. The species richness was obtained by counting the observed number of species in the resampled OTU table, and the Shannon diversity index was calculated according to the abundance of species using the 'vegan' package in R (v.3.6.1). Pearson's correlation coefficient was used to evaluate the relationship between cumulative SOC mineralisation and soil chemical properties, SOC storage and indicators of microbial community structure. Non-metric multidimensional scaling (NMDS) plots representing the differences among treatments in soil microbial community structure were prepared using Bray-Curtis distances obtained using the 'Vegan' package in R (v.3.6.1). Redundancy analysis (RDA), based on Monte Carlo permutation tests (999 permutations), was also employed using the R package 'vegan'. Path analyses were used to assess the hypothetical pathways by which soil physicochemical and microbial properties might explain SOC mineralisation. In these analyses, the data were fit to the model using maximum likelihood estimation. Path analyses were performed using the SPSS Amos 22 modelling software (IBM Corp., USA). All remaining statistical analyses were performed using SPSS v. 19.0 (IBM Corp., USA), Sigmaplot v. 12.5 (Systat Software Inc., USA), and R v. 3.6.1 (http://www.Rproject.org).

3. Results

3.1. Responses of soil chemical properties and plant biomass to imbalanced N–P input

Soil pH increased with increases in the N–P input ratio, although not significantly (Fig. 1a). All the N-P input treatments reduced soil salinity, the lowest salinity was observed in the 5:1 treatment, which was significantly lower than that in the 15:1 or 45:1 treatment (Fig. 1b). Soil IN and MBN contents increased significantly with increasing N–P input ratios (Fig. 1c and d). N-P input significantly promoted AP content. However, the differences among the three N-P input ratio treatments were not significant (Fig. 1e). Compared with the control, soil TC concentrations significantly increased and decreased in the 5:1 and 45:1 treatments, respectively, while there was no significant difference between the 15:1 treatment and the control (Fig. 1f). Plant biomass was used as an indicator of the response of plant growth to imbalanced N-P input. On the whole, N-P input significantly stimulates plant biomass. Besides, plant biomass first increased and then decreased as the N-P input ratio increased (Fig. 2.).
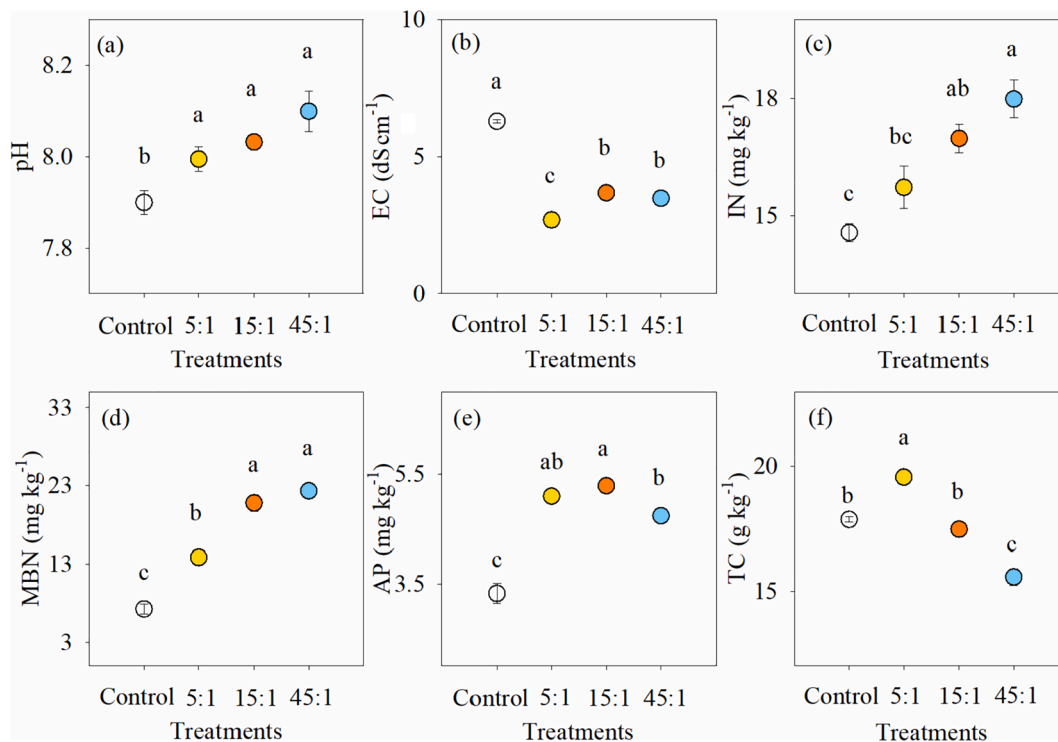
Fig. 1. Effect of imbalanced N-P input ratio on soil pH (a), salinity (b), IN (c), AP (d), MBN (e) TC (f) in a salt marsh in the YRD. Significances are indicated by lower-case letters ($p < 0.05$). Dots show the means ± SE and the vertical bars indicate standard error (n = 4).
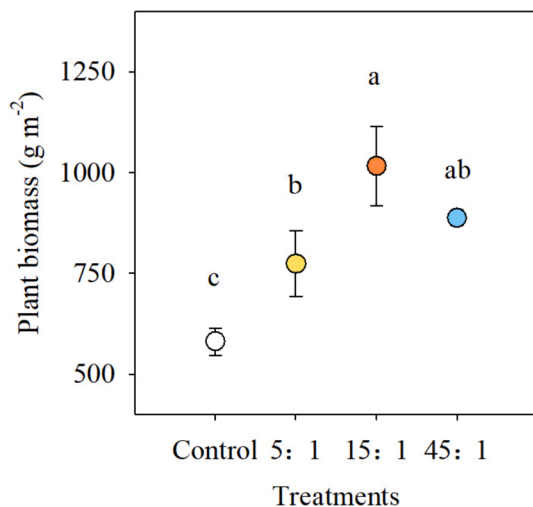

Fig. 2. Effect of imbalanced N-P input ratio on the three-year average of plant biomass in a salt marsh in the YRD. The vertical bars indicate standard error (n = 4). Different lower-case letters indicate significant difference between different N-P input ratios ($p < 0.05$).

3.2. Response of soil microbial community structure to imbalanced N–P input

The prevalent classes of bacteria in all treatment soils included *Proteobacteria*, *Gemmatimonadetes*, *Anaerolineae*, *Acidobacteria*, *Cytophagia*, *Acidimicrobiia* (Fig. 3, table S2). Class-level analyses revealed that the dominant bacterial classes were within the *Proteobacteria* among all four treatments (accounting for at least 34.7%). The four classes of *Proteobacteria* (α-, γ-, δ-, and β- *Proteobacteria*) were present at abundances of 11–12%, 10–15%, 10–12%, and 2–4%, respectively. Four years of nutrient input significantly increased the proportions of γ- and

δ-*Proteobacteria*. The proportion of *Acidobacteria* was significantly reduced by the input of nutrients. There was no significant difference in the species richness of soil bacteria among the four treatments (Fig. S1a). The Shannon diversity was significantly suppressed by N and P inputs, but there was no significant difference among the three N–P input ratio treatments (Fig. S1b). Both NMDS and dissimilarity analyses revealed a clear separation between the experimental control and the nutrients input treatments, while no significant difference in bacterial community structure was observed between the 5:1 and 15:1 treatments (Fig. S2 and Table S3).

3.3. Responses of SOC storage to imbalanced N–P input

The SOC concentrations in the 5:1 and 15:1 did not differ significantly from the control, while the 45:1 treatment significantly reduced SOC concentrations (Fig. 4a). Both 5:1 and 15:1 treatments significantly increased soil DOC and MBC concentrations (Fig. 4b and d). However, 45:1 treatment has no obvious effect on soil DOC and MBC when compared with no nutrient addition. In contrast, the SUVA$_{254}$ values in the nutrient input treatments were significantly lower than that in the control and the lowest SUVA$_{254}$ was found in the 15:1 treatment (Fig. 4c). Plant biomass showed no significant relationship with the SOC concentration. However, plant biomass displayed close correlation with soil DOC, SUVA$_{254}$ and MBC content. Plant biomass showed significant positive relationship with soil DOC and MBC content but negatively correlated with SUVA$_{254}$ (Fig. 8).

3.4. Response of SOC mineralisation to imbalanced N–P input

Throughout the incubation period, the mineralisation rates of SOC exhibited fundamentally coincident trends among all treatments (Fig. 5). The SOC mineralisation rates began at 0.68–1.65 mg CO_2-C kg^{-1} soil d^{-1} and peaked at 1.72–2.64 mg CO_2-C kg^{-1} soil d^{-1} after five days of incubation before decreasing gradually to 0.31–0.96 later in the study period (Fig. 5a). The cumulative amounts of SOC mineralisation
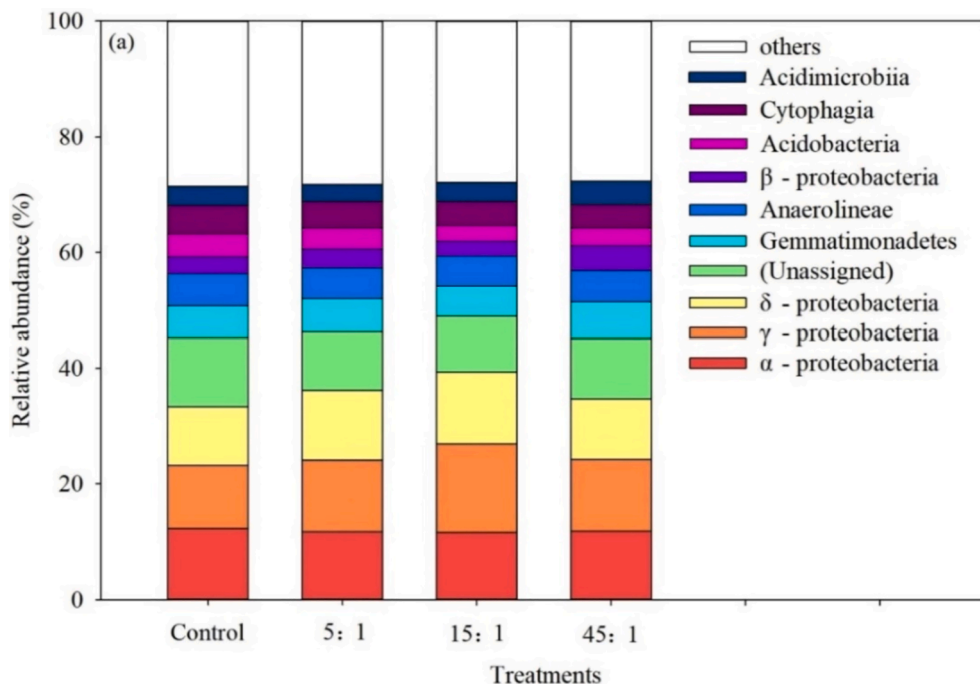
Fig. 3. Effect of imbalanced N-P input ratio on the relative abundance of the dominant soil bacterial classes in a salt marsh in the YRD. The groups with relative abundances higher than 1% are shown, while those with less than 1% relative abundance are integrated into "other". The results of one-way ANOVA analysis of the relative abundance of the dominant bacterial classes were showed in Table S1.
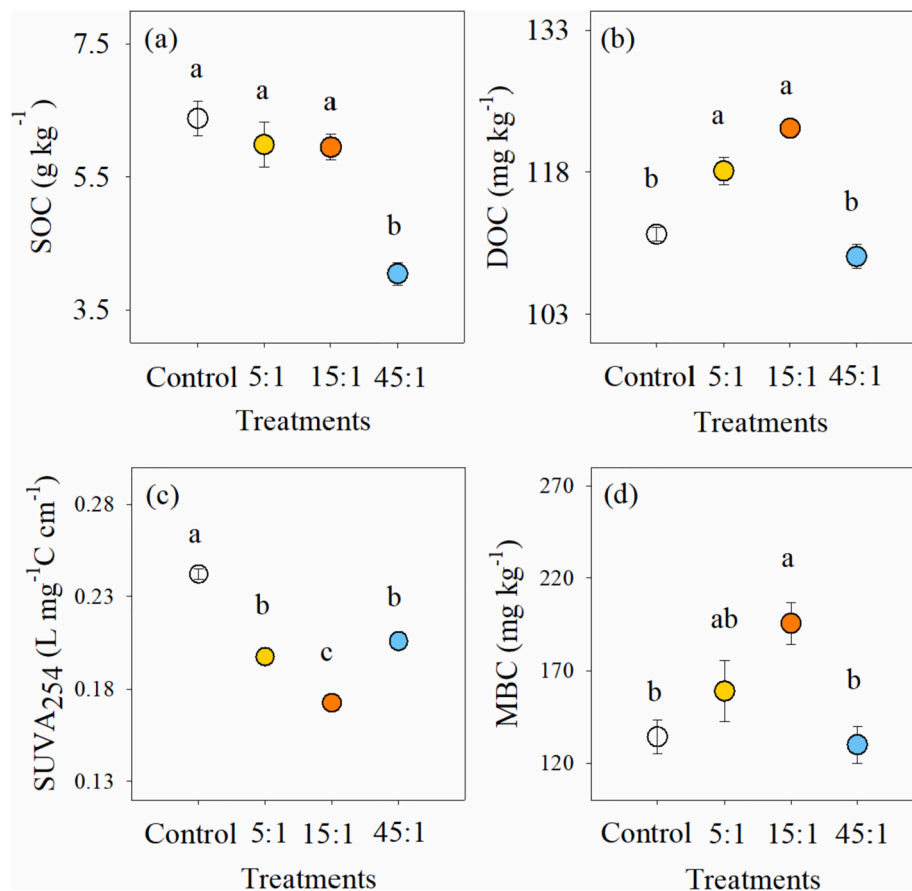

Fig. 4. Effect of imbalanced N-P input ratio on SOC (a), DOC (b), SUVA$_{254}$ (c) and MBC (d) in a salt marsh in the YRD. Significances are indicated by lower-case letters ($p < 0.05$). Dots show the means ± SE and the vertical bars indicate standard error (n = 4).
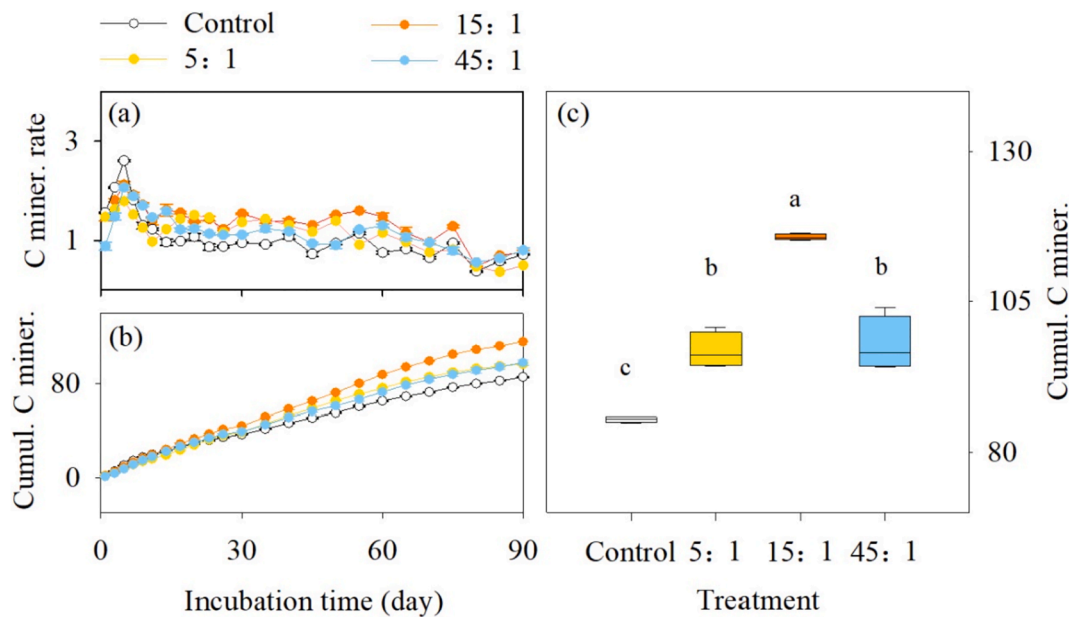
Fig. 5. (a) and (b) Dynamics of soil organic carbon (SOC) mineralization rate (C miner. Rate, mg CO_2-C kg^{-1} soil d^{-1}) and cumulative SOC mineralization (Cumul. C miner, mg CO_2-C kg^{-1} soil) over time during the 90-day incubation across all treatments. Bars indicate standard errors of the mean (in most cases smaller than the symbol); (c) Effect of imbalanced N-P input ratio on cumulative SOC mineralization (mg CO_2-C kg^{-1} soil) in a salt marsh in the YRD. Significances are indicated by lower-case letters ($p < 0.05$). Vertical bars indicate standard error (n = 4).

during the 90-day incubation of nutrient input treatments were 96.75 ± 1.49, 115.71 ± 0.25, and 97.73 ± 2.29 mg CO_2-C kg^{-1} soil in the 5:1, 15:1, and 45:1 treatments, respectively, significantly higher than the control (Fig. 5b and c).

Soil salinity displayed a negative linear correlation with SOC mineralisation, while soil IN and MBN concentrations were linearly and positively correlated with SOC mineralisation. The relationship between the mineralisation of SOC and soil AP concentrations was relatively closely fit by a quadratic equation. Cumulative SOC mineralisation increased linearly with soil DOC and MBC concentrations but decreased linearly with $SUVA_{254}$ (Fig. 6).

The path analysis model explained 90% of the variation in SOC mineralisation (Fig. 7). Increasing N–P input ratios significantly increased both the availability of soil N and the pH but had no significant impact on the availability of P. Furthermore, the N–P input ratio had

significant direct and indirect impacts on soil DOC and MBN concentrations. Soil DOC concentration was positively correlated with soil MBC and soil MBC was positively correlated with the relative abundance of γ-*Proteobacteria*. Combined, the MBC, DOC, MBN, and relative abundance of γ-*Proteobacteria* explained 96% of the variation in SOC mineralisation, which may demonstrate that the availability of C and N and the abundance of γ-*Proteobacteria* jointly controlled SOC mineralisation in our study. Pearson's correlation analysis revealed that soil AP, MBN, DOC, MBC, and the relative abundances of γ-, δ-*Proteobacteria* had significantly positive correlations with the cumulative SOC mineralisation. In contrast, soil salinity, $SUVA_{254}$, the richness of soil bacteria, and the relative abundance of *Acidobacteria* had significantly negative correlations with the cumulative SOC mineralisation (Fig. 8).
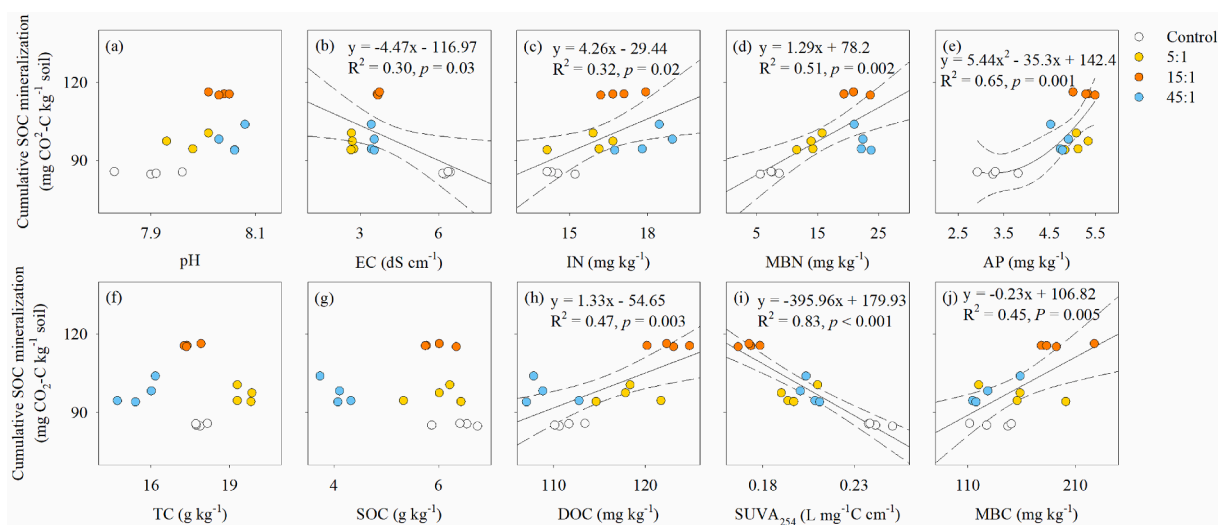

Fig. 6. Regressions of SOC mineralization cumulation with soil chemical properties and carbon fractions. Symbols indicate different N-P input ratio. Dash lines indicate the bounds of the 95% confidence intervals for regression equations. R^2 indicates coefficient of determination for the regression equation.
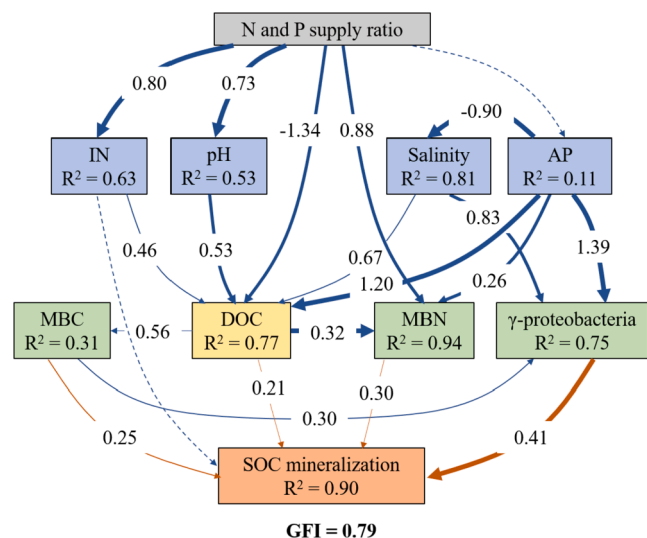
Fig. 7. The path analysis model considered the underlying causal relationships among soil organic carbon mineralization, soil physio-chemical properties, soil microbial biomass, and soil microbial abundance under different N-P input ratio treatments. GFI, goodness of fit index. Physio-chemical properties are shown in blue, soil carbon in yellow, microbial properties in green, and SOC mineralization in orange. The brown arrows are the direct effect environmental and microbial variables on SOC mineralization, and the blue arrows indicate the indirect path, respectively; dashed-line arrows indicate nonsignificant relationships ($p > 0.05$). The numbers listed within arrows are the standardized path coefficients, and the arrow width is proportional to the strength of the relationship. The R^2 values below the response variables indicate the proportion of variation explained by the relationships with other variables. IN (Inorganic nitrogen); AP (Available phosphorus); DOC (Dissolved organic carbon); MBC (Microbial biomass carbon); MBN (Microbial biomass nitrogen); γ-Proteobacteria (Relative abundance of γ-Proteobacteria). (For interpretation of the references to colour in this figure legend, the reader is referred to the web version of this article.)

4. Discussion

4.1. Effects of N–P input ratio on soil properties, plant biomass and microbial communities

Soil salinity decreased after four-years of N and P input, especially in the low N-P input ratio treatments. we considered that N-P input induced changes in soil salinity was strongly related with the variation of plant biomass. With the increase in plant biomass, the soil salinity might decrease because of reduced soil water evaporation (Shaygan et al., 2018; Qu et al., 2018; Zhao et al., 2020). Contrastingly, soil salinity might also increase due to transpiration and more water uptake by root with increased plant biomass (Chen et al., 2019a, 2019b). Thereby, soil salinity decreased along with increasing plant biomass when the plant biomass was relatively low, however, soil salinity increased when the plant biomass exceeds a certain value. The slight increase in soil pH induced by N-P input was consistent with a previous study in the YRD (Qu et al., 2020), which could be caused by P input in present study (Rasool et al., 2021). Soil IN and MBN concentrations were increases with increasing N-P input ratio. Promoting the availability of soil-active N is helpful for easing N-limitation, which may help stimulate plant growth and change soil microbial activities (Peng et al., 2019; Wei et al., 2020). The concentration of soil AP increased after the long-term input of nutrients but the N–P input ratio had only a slight impact on AP concentrations, which is inconsistent with reports from a previous study (Schleuss et al., 2019). Soil TC was strongly and positively correlated with SOC and the highest reduction of SOC in 45: 1 treatment was coupled with the highest reduction of TC. The results demonstrated that the changes in SOC was the main reason of the variation in TC.

N-P input positively affects plant growth in a nutrient poor salt marsh (Fig. 2.). Notably, the medium (15:1) N-P input treatment showed the highest plant biomass in the field experiment. A recent *meta*-analysis reported that appropriate N and P input stimulate plant growth while the high N-P input ratio always inhibit plant growth (Peng et al., 2019). This is because the imbalanced N and P input are expected to attenuate the nutrient cycling and shift ecosystems from N limitation toward P limitation (Peñuelas et al., 2013; Peng et al., 2019). At low N-P input ratio, N input can promote soil P availability and thus plant growth.
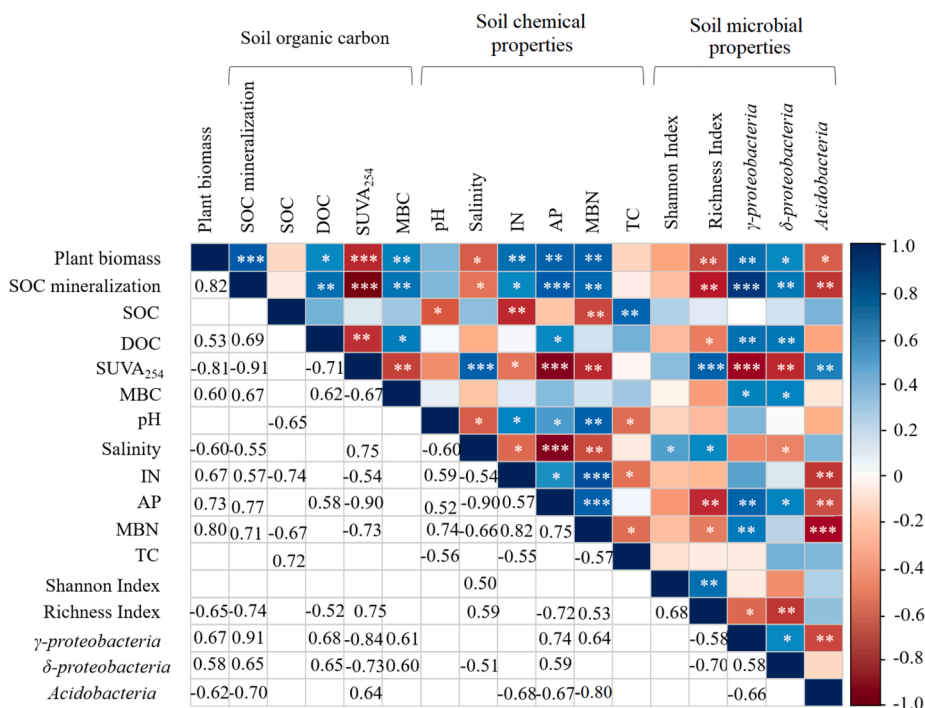

Fig. 8. Pearson correlations among plant biomass (mean value of three years), SOC mineralization cumulations, soil carbon fractions, soil chemical properties and soil microbial properties under different N-P input ratio treatments. The symbols *, ** and *** indicate significant correlations at the 0.05, 0.01 and 0.001 levels, respectively (n = 16). The numbers in the small squares indicate correlation coefficient between the two parameters. The right axis is the legend, on which correlation coefficient values are represented by different colors.

However, as N-P ratio continues to increase, the P availability is not enough to balance the growing P requirement (Li et al. 2016), and P limitation may be strengthened (Peñuelas et al. 2013). Thereby, we proposed that the excessive N induced P limitation weakened the positive response of plant growth to N-P input in the present study.

N and P input ratio also changed the structure of soil microbial communities. The N–P input ratio had a significant impact on the *β-diversity* but not α-diversity of soil microbial communities, indicating that the N–P input ratio greatly impacts the composition rather than the number of species present in soil bacterial communities. In this present study, *Proteobacteria* dominated the salt marsh and the abundance of *γ*- and *δ-Proteobacteria* and *Acidobacteria* exhibited changes among the nutrient input treatments (Fig. 3, table S2), that were consistent with the result of another recent study (Tahovska et al., 2020). The results suggest that *Proteobacteria* and *Acidobacteria* may play important roles in the salt marsh under various N–P input ratios (Fierer et al., 2012; Mannisto et al., 2016). Decreased C/N ratios of microbial biomass are generally considered to indicate a microbial community with a greater abundance of taxa with better high-N adaptability, greater energy demands, and faster growth and turnover (Tahovska et al., 2020; Vanveen et al., 1984). Accordingly, the relative abundance of some copiotrophic taxa including *γ*- and *δ-Proteobacteria* were higher in the nutrient input treatments and highest in the medium input treatments (15:1). Conversely, the relative abundance of *Acidobacteria*, an oligotrophic taxon, was lower in the nutrient input treatments (Fig. 3a, Table S2). The results of sequence analyses showed that the input of N and P, especially in the medium input ratio treatment, alleviated the nutrient stress of bacteria under oligotrophic conditions.

4.2. Effects of N–P input ratio on SOC storage

The accumulation of SOC depends on both input and loss of SOC. The processes involved in the SOC cycling can be strongly driven by biotic and abiotic factors including the establishment of vegetation, decomposition of SOC and leaching, etc. Previous studies have shown that low level input of N and P enhance SOC storage in nutrients limited ecosystems (Jian et al., 2016; Pastore et al., 2017). Other studies have shown that long-term N enrichment induces P limitation, which restricts vegetative biomass and reduces C accumulation (Stiles et al., 2017). Our results supported these ideas and showed that the effects on SOC content and fractions are strongly dependent on the N-P input ratio. While SOC mineralisation was strongly promoted by nutrients input when the N–P input ratio was < 15:1, the SOC contents were not significantly different among the low (5:1) and medium (15:1) treatments and the control. However, while an excessively high N–P input ratio suppressed SOC mineralisation, SOC concentration still declined, indicating that there may be an N–P input ratio threshold between 15:1 to 45:1, such that below this threshold, the SOC pool can maintain a dynamic balance, while above this threshold, the SOC pool would shift sharply from a C sink to a C source. Similar results were obtained in a temperate, needle–broadleaved forest (Cheng et al., 2017).

DOC is usually considered to represent the amount of soluble SOC. It plays a critical role in wetlands because it is labile and easily leached (Majidzadeh et al., 2017). Our results showed that the soil DOC contents in the 5:1 and 15:1 treatments were higher than in the control. DOC is mainly deriving from aboveground litter, the root exudates of plants, and primary decomposition of SOC (Mao et al., 2017; Zsolnay, 2003). Thus, the effects of N–P input ratio on the production of DOC is likely driven by two factors. First, the changes of plant biomass under different N-P input ratio led to DOC variation. The primary productivity controlled by the plant aboveground biomass, meanwhile, the photosynthetic C was transported to soil through the root. Therefore, N-P input increased DOC input through stimulated plant biomass. Some other studies also suggested that an excessive dose of N can induce P limitation that leads to lower root biomass, weaker rhizodeposition and less DOC input (Janssens et al., 2010; Peng et al., 2019). Secondly, prior

works have shown that a small amount of added N can lead to an increase in DOC leaching from mineral soils by promoting soil pH (Evans et al., 2008; Pregitzer et al., 2004). The results of path analysis in this study confirmed the relationship between soil DOC and pH under N and P input (Fig. 7). However, other studies have reported inconsistent results (Chang et al., 2018; Hagedorn et al., 2012). Therefore, further research is needed to support these inferences.

The effect of the N–P input ratio on the $SUVA_{254}$ of DOC was almost opposite to that on the soil DOC content. As $SUVA_{254}$ is widely used as an indicator of the recalcitrant aromatic component of DOC (Liu et al., 2017; Wang et al., 2015), the results of our study indicate that the low and medium N–P input ratio not only increased the soil DOC, but also suppressed the relative proportion of aromatic compounds. Thus, the relatively low N–P input ratio stimulated microbial activities by increasing labile SOC components, thereby promoting the loss of SOC via decomposition, which was also confirmed in our laboratory experiment.

Low and medium N–P input ratios caused a significant increase in soil MBC, but the high input ratio has no obvious effect. The result agreed with a previous study in which MBC declined in a mesic grassland due to increasing N–P input ratio (Schleuss et al., 2019). Soil MBC is the most active and easily obtained component in soil organic matter, which is a driving force for the decomposition of soil organic matter by microorganisms (Chen et al., 2019a, 2019b; Schleuss et al., 2019). One explanation for this is that the low and medium N–P input ratio positively affected soil microbial activities and biomass by promoting nutrient availability and increasing root rhizodeposition (Janssens et al., 2010). These was supported by the correlation analysis, which showed significant positive relationships of soil MBC with plant biomass and soil DOC in this research.

4.3. Effects of N–P input ratio on SOC mineralisation in laboratory incubations

The SOC mineralisation did not increase linearly with the increasing input ratio of N and P. The maximum SOC mineralisation was observed in the medium N–P input ratio treatments. We found that input of N and P decreased soil salinity by 40–60% (Fig. 1b), indicating that nutrient input may relieve salt stress on soil microorganisms (Qu et al., 2018; Yang et al., 2018). Additionally, our results revealed that SOC mineralisation in this salt marsh is co-limited by N and P and the medium N-P input ratio was the most favorable for SOC mineralisation. Wei et al. (2020) found that the addition of N or P alone aggravated the limitation of the other nutrient on soil microorganisms. Moreover, regression and path analysis showed that SOC mineralisation was directly controlled by soil MBC and DOC contents in the present study (Fig. 4), which is consistent with the findings in prior works demonstrated that heterotrophic soil communities are inherently C-limited, especially in nutrient-rich environments (Chen et al., 2018; Soong et al., 2020). Previous studies have also shown that excessive N input would greatly increase soil NH_4^+. The cation toxicity of high NH_4^+ might decrease P uptake and limit plant growth, thereby suppressing the input of new labile C and the decomposition of SOC in wetland ecosystems (Nihlgård, 1985; Wei et al., 2013; Zhang et al., 2014; Peng et al., 2019; Wang et al., 2019).

N and P input had been shown to disturb microbial growth and activities and greatly influence SOC mineralisation (Xiao et al., 2017; Yang et al., 2018). Our results showed that the soil microbial communities in the nutrient input treatments had more biomass at lower C/N ratios, when compared to those in the control soil. According to our path analysis, SOC mineralisation was significantly and positively correlated with soil MBC. It has been noted in many studies that the addition of nutrients may greatly affects the stoichiometry of microbial biomass due to changes in availability of nutrients (Chen et al., 2018; Tahovska et al., 2020; Zhou et al., 2017). A lower C/N ratio of microbial biomass is often observed with higher respiration rates (Tahovska et al., 2020). Moreover, previous studies have shown that changes in plant productivity

and the allocation of C likely cause variations in MBC (Dong et al., 2020). The relationships between plant biomass and MBC in our research serves to confirm this view.

Compositional changes in microbial community structures directly impact the mineralisation of SOC. In this study, we found that all three N-P input treatments stimulated SOC mineralisation compared with no N-P input treatment, and the greatest effect was observed in the medium N–P input ratio treatments. These results indicate that the metabolic activities of microbial populations that dominate SOC mineralisation were amplified in the medium treatments, while the low and high N–P input ratios decreased their adaptability (Tahovska et al., 2020). Similar results have been reported in grassland and forest ecosystems, which have revealed that imbalanced N–P ratios reduce the bioavailability of soil nutrients and weaken the ability of microbes to decompose SOC (Vanveen et al., 1984; Wei et al., 2020).

5. Conclusions

This study made progress towards investigating mechanisms of nonlinear responses in soil C storage and SOC mineralisation to imbalanced N-P input in a salt marsh in the YRD. Excessive N-P input ratio would trigger SOC loss, while low N-P input ratio has no effects on SOC. Given a large rise in the ratio of N–P input in the future, higher N–P input ratios may cause the salt marshes to shift from soil C sinks to soil C sources. Appropriate N-P input ratio increased soil DOC and MBC and decreased the aromatic DOC components through improving the plant growth. The SOC mineralisation was first increased and then decreased with increasing N-P input ratio. N–P input ratios regulated SOC mineralisation by changing labile SOC fractions and microbial community structures. Our results may be used to better understand how imbalanced N-P inputs impact SOC accumulation in coastal wetland ecosystems.

Declaration of Competing Interest

The authors declare that they have no known competing financial interests or personal relationships that could have appeared to influence the work reported in this paper.

Acknowledgements

This research was funded by the Strategic Priority Research Program of the Chinese Academy of Sciences (XDA23050202), the National Natural Science Foundation of China (42071126), International Science Partnership Program of the Chinese Academy of Sciences (121311KYSB20190029), and Natural Science Foundation of Shandong Province (ZR2019BC106). We are grateful for the support from Yellow River Delta Ecological Research Station of Coastal Wetland, CAS.

Appendix A. Supplementary data

Supplementary data to this article can be found online at https://doi.org/10.1016/j.catena.2021.105720.

References

Cao, Z., Jia, Y., Cai, Y., Wang, X., Hu, H., Zhang, J., Jia, J., Feng, X., 2019. Past aridity's effect on carbon mineralization potentials in grassland soils. Biogeosciences 16, 3605–3619.
Chang, R., Li, N., Sun, X., Hu, Z., Wang, G., 2018. Nitrogen addition reduces dissolved organic carbon leaching in a montane forest. Soil Biol. Biochem. 127, 31–38.
Chen, Q., Wang, Y., Zou, C., Wang, Z., 2017. Aboveground Biomass Invariance Masks Significant Belowground Productivity Changes in Response to Salinization and Nitrogen Loading in Reed Marshes. Wetlands 37, 985–995.
Chen, H., Li, D., Zhao, J., Zhang, W., Xiao, K., Wang, K., 2018. Nitrogen addition aggravates microbial carbon limitation: Evidence from ecoenzymatic stoichiometry. Geoderma 329, 61–64.
Chen, X., Hao, B., Jing, X., He, J.-S., Ma, W., Zhu, B., 2019a. Minor responses of soil microbial biomass, community structure and enzyme activities to nitrogen and phosphorus addition in three grassland ecosystems. Plant Soil 444, 21–37.
Chen, Z., Sun, S., Zhu, Z., Jiang, H., Zhang, X., 2019b. Assessing the effects of plant density and plastic film mulch on maize evaporation and transpiration using dual crop coefficient approach. Agricultural Water Management 225, 105765.
Cheng, S., Fang, H., Yu, G., 2017. Threshold responses of soil organic carbon concentration and composition to multi-level nitrogen addition in a temperate needle-broadleaved forest. Biogeochemistry 137, 219–233.
Chmura, G.L., Anisfeld, S.C., Cahoon, D.R., Lynch, J.C., 2003. Global carbon sequestration in tidal, saline wetland soils. Glob. Biogeochem. Cycle 17, 1111.
Davies, T., Lovelock, C., Pettit, N., Grierron, P., 2017. Short-term microbial respiration in an arid zone mangrove soil is limited by availability of gallic acid, phosphorus and ammonium[J]. Soil Biol. Biochem 115, 73–81.
Deegan, L., Johnson, D., Warren, R., Peterson, B., Fleeger, J., Fagherazzi, S., Wollheim, W., 2012. Coastal eutrophication as a driver of salt marsh loss. Nature 490, 388–392.
Dong, J., Wang, S., Niu, H., Cui, X., Li, L., Pang, Z., Zhou, S., Wang, K., 2020. Responses of soil microbes and their interactions with plant community after nitrogen and phosphorus addition in a Tibetan alpine steppe.J. Soils Sediments 20, 2236–2247.
Evans, C.D., Goodale, C.L., Caporn, S.J.M., Dise, N.B., Emmett, B.A., Fernandez, I.J., Field, C.D., Findlay, S.E.G., Lovett, G.M., Meesenburg, H., 2008. Does elevated nitrogen deposition or ecosystem recovery from acidification drive increased dissolved organic carbon loss from upland soil? A review of evidence from field nitrogen addition experiments. Biogeochemistry 91, 13–35.
Fierer, N., Lauber, C.L., Ramirez, K.S., Zaneveld, J., Bradford, M.A., Knight, R., 2012. Comparative metagenomic, phylogenetic and physiological analyses of soil microbial communities across nitrogen gradients. ISME J.6, 1007–1017.
Gao, Q., Hasselquist, N.J., Palmroth, S., Zheng, Z., You, W., 2014. Short-term response of soil respiration to nitrogen fertilization in a subtropical evergreen forest. Soil Biol. Biochem. 76, 297–300.
Guesewell, S., Gessner, M.O., 2009. N : P ratios influence litter decomposition and colonization by fungi and bacteria in microcosms. Funct. Ecol. 23, 211–219.
Gusewell, S., 2005. Responses of wetland graminoids to the relative supply of nitrogen and phosphorus. Plant Ecol. 176, 35–55.
Hagedorn, F., Kammer, A., Schmidt, M.W.I., Goodale, C.L., 2012. Nitrogen addition alters mineralization dynamics of ^{13}C-depleted leaf and twig litter and reduces leaching of older DOC from mineral soil. Glob. Change Biol. 18, 1412–1427.
Han, G., Sun, B., Chu, X., Xing, Q., Song, W., Xia, J., 2018. Precipitation events reduce soil respiration in a coastal wetland based on four-year continuous field measurements. Agric. For. Meteorol. 256–257, 292–303.
Hasselquist, N.J., Metcalfe, D.B., Hogberg, P., 2012. Contrasting effects of low and high nitrogen additions on soil CO$_2$ flux components and ectomycorrhizal fungal sporocarp production in a boreal forest. Glob. Change Biol. 18, 3596–3605.
Hill, T.D., Roberts, B.J., 2017. Effects of seasonality and environmental gradients on Spartina alterniflora allometry and primary production. Ecol Evol. 7, 9676–9688.
Janssens, I.A., Dieleman, W., Luyssaert, S., Subke, J.A., Reichstein, M., Ceulemans, R., Ciais, P., Dolman, A.J., Grace, J., Matteucci, G., Papale, D., Piao, S.L., Schulze, E.D., Tang, J., Law, B.E., 2010. Reduction of forest soil respiration in response to nitrogen deposition. Nat. Geosci. 3, 315–322.
Jian, S., Li, J., Ji, C., Wang, G., Mayes, M.A., Dzantor, K.E., Hui, D., Luo, Y., 2016. Soil extracellular enzyme activities, soil carbon and nitrogen storage under nitrogen fertilization: A meta-analysis. Soil Biol. Biochem. 101, 32–43.
Kalbitz, K., Schmerwitz, J., Schwesig, D., Matzner, E., 2003. Biodegradation of soil-derived dissolved organic matter as related to its properties. Geoderma. 113, 273–291.
Kirwan, M.L., Mudd, S.M., 2012. Response of salt- marsh carbon accumulation to climate change. Nature. 489, 550–553.
Koerselman, W., Meuleman, A.F.M., 1996. The vegetation N: P ratio: A new tool to detect the nature of nutrient limitation. J. Appl. Ecol. 33, 1441–1450.
Li, Y., Niu, S.L., Yu, G.R., 2016. Aggravated phosphorus limitation on biomass production under increasing nitrogen loading: a meta-analysis. Glob. Chang. Biol. 22, 934–943.
Li, X., Chen, H., Jiang, X., Yu, Z., Yao, Q., 2017. Impacts of human activities on nutrient transport in the Yellow River: The role of the Water-Sediment Regulation Scheme. Sci. Total Environ. 592, 161–170.
Liu, X., Ruecker, A., Song, B., Xing, J., Conner, W.H., Chow, A.T., 2017. Effects of salinity and wet–dry treatments on C and N dynamics in coastal-forested wetland soils: Implications of sea level rise. Soil Biol. Biochem. 112, 56–67.
Liu, X., Wang, G., Ran, Y., Qi, D., Han, G., Guan, B., Hao, C., 2019. Overall supply level, not the relative supply of nitrogen and phosphorus, affects the plant community composition of a supratidal wetland in the Yellow River Delta. Sci. Total Environ. 695, 133866.
Luo, X., Mazer, S.J., Guo, H., Zhang, N., Weiner, J., Hu, S., 2016. Nitrogen: phosphorus supply ratio and allometry in five alpine plant species. Ecol. Evol. 6, 8881–8892.
Majidzadeh, H., Uzun, H., Ruecker, A., Miller, D., Vernon, J., Zhang, H., Bao, S., Tsui, M. T.K., Karanfil, T., Chow, A.T., 2017. Extreme flooding mobilized dissolved organic matter from coastal forested wetlands. Biogeochemistry 136, 293–309.
Mannisto, M., Ganzert, L., Tiirola, M., Haggblom, M.M., Stark, S., 2016. Do shifts in life strategies explain microbial community responses to increasing nitrogen in tundra soil? Soil Biol. Biochem. 96, 216–228.
Mao, R., Zhang, X.-H., Li, S.-Y., Song, C.-C., 2017. Long-term phosphorus addition enhances the biodegradability of dissolved organic carbon in a nitrogen-limited temperate freshwater wetland. Sci. Total Environ. 605, 332–336.

Nellemann, C., Corcoran, E., Duarte, C., Valdés, L., Young, C.D., Fonseca, L., Grimsditch, G., 2009. Blue carbon: the role of healthy oceans in binding carbon: a rapid response assessment. GRID- Arendal, Arendal, Norway, pp. 589–598.

Nie, M., Zhang, X., Wang, J., Jiang, L., Yang, J., Quan, Z., Cui, X., Fang, C., Li, B., 2009. Rhizosphere effects on soil bacterial abundance and diversity in the Yellow River Deltaic ecosystem as influenced by petroleum contamination and soil salinization. Soil Biol. Biochem. 41, 2535–2542.

Nihlgård, B., 1985. The ammonium hypothesis:an additional explanation to the forest dieback in europe. Ambio 14, 2–8.

Pascault, N., Ranjard, L., Kaisermann, A., Bachar, D., Christen, R., Terrat, S., Mathieu, O., Leveque, J., Mougel, C., Henault, C., Lemanceau, P., Pean, M., Boiry, S., Fontaine, S., Maron, P.-A., 2013. Stimulation of different functional groups of bacteria by various plant residues as a driver of soil priming effect. Ecosystems 16, 810–822.

Pastore, M.A., Megonigal, J.P., Langley, J.A., 2017. Elevated CO_2 and nitrogen addition accelerate net carbon gain in a brackish marsh. Biogeochemistry 133, 73–87.

Peng, Y., Peng, Z., Zeng, X., Houx III, J.H., 2019. Effects of nitrogen-phosphorus imbalance on plant biomass production: a global perspective. Plant Soil 436, 245–252.

Peñuelas, J., Poulter, B., Sardans, J., Ciais, P., van der Velde, M., Bopp, L., Boucher, O., Godderis, Y., Hinsinger, P., Llusia, J., Nardin, E., Vicca, S., Obersteiner, M., Janssens, I.A., 2013. Human-induced nitrogen-phosphorus imbalances alter natural and managed ecosystems across the globe. Nat, Commun, p. 4.

Pregitzer, K.S., Zak, D.R., Burton, A.J., Ashby, J.A., MacDonald, N.W., 2004. Chronic nitrate additions dramatically increase the export of carbon and nitrogen from northern hardwood ecosystems. Biogeochemistry 68, 179–197.

Qu, W., Li, J., Han, G., Wu, H., Song, W., Zhang, X., 2018. Effect of salinity on the decomposition of soil organic carbon in a tidal wetland. J. Soils Sediments 19, 609–617.

Qu, W., Han, G., Eller, F., Xie, B., Wang, J., Wu, H., Li, J., Zhao, M., 2020. Nitrogen input in different chemical forms and levels stimulates soil organic carbon decomposition in a coastal wetland. Catena. 194, 104672.

Ramirez, K.S., Craine, J.M., Fierer, N., 2012. Consistent effects of nitrogen amendments on soil microbial communities and processes across biomes. Glob. Change Biol. 18, 1918–1927.

Rasool, B., Mahmoodur-Rahman, Ramzani, P., Zubair, M., Iqbal, M., 2021. Impacts of oxalic acid-activated phosphate rock and root-induced changes on lead bioavailability in rhizosphere and distribution in mung bean plant. Environmental Pollution, 280, 116903.

Schleuss, P.-M., Widdig, M., Heintz-Buschart, A., Guhr, A., Martin, S., Kirkman, K., Spohn, M., 2019. Stoichiometric controls of soil carbon and nitrogen cycling after long-term nitrogen and phosphorus addition in a mesic grassland in South Africa. Soil Biol. Biochem. 135, 294–303.

Shaygan, M., Mulligan, D., Baumgartl, T., 2018. The potential of three halophytes (Tecticornia pergranulata, Sclerolaena longicuspis, and Frankenia serpyllifolia) for the rehabilitation of brine-affected soils. Land Degrad. Dev. 29, 2002–2014.

Sonmez, O., Turan, V., Kaya, C., 2016. The effects of sulfur, cattle, and poultry manure addition on soil phosphorus. Turk. J. Agric. For. 40, 536–541.

Soong, J.L., Fuchslueger, L., Maranon-Jimenez, S., Torn, M.S., Janssens, I.A., Penuelas, J., Richter, A., 2020. Microbial carbon limitation: The need for integrating microorganisms into our understanding of ecosystem carbon cycling. Glob, Change Biol, p. 26.

Stiles, W.A.V., Rowe, E.C., Dennis, P., 2017. Long-term nitrogen and phosphorus enrichment alters vegetation species composition and reduces carbon storage in upland soil. Sci. Total Environ. 593, 688–694.

Sun, Y., Peng, S., Goll, D.S., Ciais, P., Guenet, B., Guimberteau, M., Hinsinger, P., Janssens, I.A., Penuelas, J., Piao, S., 2017. Diagnosing phosphorus limitations in natural terrestrial ecosystems in carbon cycle models. Earths Future 5, 730–749.

Tahovska, K., Choma, M., Kastovska, E., Oulehle, F., Barta, J., Santruckova, H., Moldan, F., 2020. Positive response of soil microbes to long-term nitrogen input in spruce forest: Results from Gardsjon whole-catchment N-addition experiment. Soil Biol. Biochem. 143, 107732.

Vance, E.D., Brookes, P.C., Jenkinson, D.S., 1987. An extraction method for measuring soil microbial biomass C. Soil Biol. Biochem. 19, 703–707.

Vanveen, J.A., Ladd, J.N., Frissel, M.J., 1984. Modeling C and N turnover through the microbial biomass in soil. Plant Soil 76, 257–274.

Vesterdal, L., Elberling, B., Christiansen, J.R., Callesen, I., Schmidt, I.K., 2012. Soil respiration and rates of soil carbon turnover differ among six common European tree species. For. Ecol. Manage. 264, 196.

Wang, J.-J., Dahlgren, R.A., Chow, A.T., 2015. Controlled burning of forest detritus altering spectroscopic characteristics and chlorine reactivity of dissolved organic matter: Effects of temperature and oxygen availability. Environ. Sci. Technol. 49, 14019–14027.

Wang, J., Gao, Y., Zhang, Y., Yang, J., Smith, M.D., Knapp, A.K., Eissenstat, D.M., Han, X., 2019. Asymmetry in above- and belowground productivity responses to N addition in a semi-arid temperate steppe. Glob. Change Biol. 25, 2958–2969.

Wei, C., Yu, Q., Bai, E., Lü, X., Li, Q.I., Xia, J., Han, X., 2013. Nitrogen deposition weakens plant-microbe interactions in grassland ecosystems. Glob. Chang. Biol. 19, 3688–3697.

Wei, S., Tie, L., Liao, J., Liu, X., Du, M., Lan, S., Li, X., Li, C., Zhan, H., Huang, C., 2020. Nitrogen and phosphorus co-addition stimulates soil respiration in a subtropical evergreen broad-leaved forest. Plant Soil 450, 171–182.

Wieder, W.R., Allison, S.D., Davidson, E.A., Georgiou, K., Hararuk, O., He, Y., Hopkins, F., Luo, Y., Smith, M.J., Sulman, B., Todd-Brown, K., Wang, Y.-P., Xia, J., Xu, X., 2015. Explicitly representing soil microbial processes in Earth system models. Glob. Biogeochem. Cycle 29, 1782–1800.

Xiao, L., Xie, B., Liu, J., Zhang, H., Han, G., Wang, O., Liu, F., 2017. Stimulation of long-term ammonium nitrogen deposition on methanogenesis by Methanocellaceae in a coastal wetland. Sci. Total Environ. 595, 337–343.

Xiao, L.L., Wei, W.C., Luo, M., Xu, H.D., Feng, D.W., Yu, J.F., Huang, J.F., Liu, F.H., 2019. A potential contribution of a Fe(III)-rich red clay horizon to methane release: Biogenetic magnetite-mediated methanogenesis. Catena 181, 7.

Yang, J., Zhan, C., Li, Y., Zhou, D., Yu, Y., Yu, J., 2018. Effect of salinity on soil respiration in relation to dissolved organic carbon and microbial characteristics of a wetland in the Liaohe River estuary. Northeast China. Sci. Total Environ. 642, 946–953.

Yu, J., Ning, K., Li, Y., Du, S., Han, G., Xing, Q., Wu, H., Wang, G., Gao, Y., 2014. Wet and dry atmospheric depositions of inorganic nitrogen during plant growing season in the coastal zone of Yellow River Delta. Sci. World J 1–8.

Zhang, Y.H., Lü, X.T., Isbell, F., Stevens, C., Han, X., He, N.P., Zhang, G.M., Yu, Q., Huang, J.H., Han, X.G., 2014. Rapid plant species loss at high rates and at low frequency of N addition in temperate steppe. Glob. Chang. Biol. 20, 3520–3529.

Zhao, M.L., Han, G.X., Li, J.Y., Song, W.M., Qu, W.D., Eller, F., Wang, J.P., Jiang, C.S., 2020. Responses of soil CO_2 and CH_4 emissions to changing water table level in a coastal wetland. J. Cleaner. Prod. 269, 122316.

Zhou, G., Luo, Q., Chen, Y., Hu, J., He, M., Gao, J., Zhou, L., Liu, H., Zhou, X., 2019. Interactive effects of grazing and global change factors on soil and ecosystem respiration in grassland ecosystems: A global synthesis. J. Appl. Ecol. 56, 2007–2019.

Zhou, Z., Wang, C., Zheng, M., Jiang, L., Luo, Y., 2017. Patterns and mechanisms of responses by soil microbial communities to nitrogen addition. Soil Biol. Biochem. 115, 433–441.

Zsolnay, Á., 2003. Dissolved organic matter: artefacts, definitions, and functions. Geoderma 113, 187–209.